ANALYSIS OF CREEP VISCOELASTIC MECHANICAL BEHAVIOR IN BEAMS USING THE FINITE ELEMENT POSITIONAL FORMULATION

Becho, Juliano dos Santos

Rabelo, João Marcos Guimarães

De Oliveira, Paulo Gonçalves Júnior

Barros, Felício Bruzzi

Greco, Marcelo

julinobecho@dees.ufmg.br

joãomarcos@dees.ufmg.br

pauloteiu@eng.grad.ufmg.br

felicio@dees.ufmg.br

mgreco@dees.ufmg.br

Structural Engineering Graduate Program, Federal University of Minas Gerais, School of Engineering, Department of Structural Engineering. Av. Presidente Antônio Carlos, 6627 / Rom Office 4127 / Belo Horizonte – MG, Zip-Code: 31270-901, Brazil.

Abstract. *The present work addresses the issue of the nonlinear numerical analysis of beams with creep viscoelastic behavior. The numerical strategy adopted is the Finite Element nonlinear positional formulation, taking into account the classic theory of Bernoulli-Euler. The geometrical nonlinearity represented by the structural equilibrium in the deformed position is solved using the Newton-Raphson method. The physical nonlinearity refers to the adoption of a rheological relation to describe the viscoelastic behavior, deduced from a uniaxial rheological model based on the generalized Maxwell model. The formulation is fitted by using the creep results of uniaxial tension tests on Glass Fiber Reinforced Plastic, obtained from the literature. This is achieved by the parametrization of the height of the cross section is adopted, which provides an idealization of the beam as bundled bars. Then the presented formulation is used to analyze a beam with different boundary conditions. The results are used to compare the elastic and viscoelastic behaviors of the beam and to demonstrate the representative capacity of the phenomenon with the adopted formulation and fitting approach.*

Keywords: *Viscoelasticity, Creep, Positional Formulation, FEM, Rheological Model*

1 INTRODUCTION

On a structural project, one of the fundamental problems is finding a solution that presents a good performance (a predictable and safe structure) with low economic cost. With this purpose, many works have been devoted to the study and modeling of the behavior of alternative materials in many different areas, such as infrastructure, civil construction, mechanical industry, aerospace industry. The works of Godat et al. (2013), Kästner et al. (2012), Sá et al. (2011) and Muñoz-Rojas et al. (2011) are good examples.

Among other alternative materials used in recent studies, we point out the polymeric materials and the composite materials with polymeric matrix, especially for presenting a good strength/stiffness ratio in comparison to conventional structural materials. On the other hand, in general these materials present viscoelastic or viscoelastoplastic mechanical behavior depending on their properties and the stress levels they are exposed to. These behaviors are characterized by their dependence of time in response to external exposures, and are described by the combination of viscous behavior, characteristic of fluid materials, and elastic behavior, characteristic of solid materials (Findley et al., 1976).

The interests of some of the recent studies related to viscoelastic and viscoelastoplastic behavior are focused in the development of numerical formulations that adopt phenomenological equations, based on rheological models, to represent the relation between the stress, strain and time; and on parameter fitting techniques for these models, as pointed out in the following works.

Semptikovski and Muñoz-Rojas (2013) propose a tridimensional formulation of the finite elements method using a simplified beam element. In this work the linear viscoelastic behavior in elements made of high density polyethylene is considered from a generalized Maxwell rheological model, based on Kaliske and Rothert (1997).

Liu et al. (2008) propose a formulation based on integral equations for describing the nonlinear viscoelastic behavior of polyethylene for structural applications. The viscoelastic behavior is considered by adopting the generalized model of Kelvin-Voigt and the respective parameters are obtained through a methodology based on linear interpolation. A similar formulation is adopted in Kühl et al. (2013) to describe the viscoelastic behavior of high density polyethylene. The viscoelastic part of the strain, a generalized model of Kelvin-Voigt is adopted, and, for the viscoelastoplastic part, the equation of Zapas-Crissman is considered. The viscoelastic parameters are obtained through a curve fitting based on the method of particle swarm optimization, whereas the viscoplastic parameters are obtained through a linear regression of the least squares method.

Carniel et al. (2015) propose a formulation of the finite elements method to analyze spatial truss with viscoelastic and viscoelastoplastic behavior including mechanical degradation. The generalized rheological model of Kelvin-Voigt is adopted for the description of viscoelastic behavior, whereas the viscoplastic behavior is considered by using the equation of Perzyna. The degradation of the material is considered by using the damage model of Lemaitre. The parameters of the material are obtained through a curve fitting based on the particle swarm optimization.

Furthermore, some recent studies about viscoelasticity present developments related to the use of fractional derivatives to obtain simpler rheological models and with a more precise representation of the complex behavior of real materials, such as composite materials, polymeric materials, biological tissues, among others (Shen et al., 2013; Bahrani et al., 2013; Pérez Zerpa et al., 2015; Haveroth et al. 2015).

The present work is focused only on the viscoelastic mechanical behavior characterized by the strain variation over time in solid materials when exposed to constant stress, known as creep phenomenon (Marques and Creus, 2012; Christensen, 2010).

In this context the present work is dedicated to present a numerical formulation to describe the creep behavior in beams made of viscoelastic material. This description of creep behavior consists in obtaining an equilibrium position of the beams after a determined time interval, under a determined state of static load, and in the representation of the evolution of displacements over time.

To do so, the developed numerical formulation is based on the nonlinear positional formulation of the Finite Elements Method. In this work the formulation is particularly used to describe the creep mechanical behavior in plane frame finite elements taking into account the classical theory of Bernoulli-Euler and adopting an engineering strain measure.

The presented formulation is based on the work developed by Becho et al. (2015). However, differently from this one, in the present work the contribution of creep is introduced after the parametrization of the beam height. This procedure provides an idealization of the beam as a bundle of bars and allows the adoption of the generalized Maxwell uniaxial rheological model (standard solid model), when considering the relation between stress, strain and time. Furthermore, this approach allows to obtain the beam displacements increase over time, due to viscoelastic behavior, not only of the contribution calculated from the central line of the beam, but due the sum of the contributions calculated in each point distributed along its height. The main advantage of this approach, in addition to allowing a more refined analysis of the stress, is the possibility to use the creep results of uniaxial tension tests in bars when fitting the formulation in a simple way.

2 POSITIONAL FORMULATION OF THE FEM

The positional formulation of the Finite Elements Method used for this work is based on the formulation found in Coda and Greco (2004), which was originally developed to analyze plane reticulated structures with physical and geometrical nonlinearities. The method was selected due to its efficiency in the applications and developments shown in recent researches concerning the nonlinear numerical analysis, besides being supported by physics principles based on energy equilibrium that are both consistent and easy to understand.

Generally the positional formulation can be shown by Eq. (1), which represents the total potential energy (Π) of a structure exposed to external loads.

$$\Pi = U - P \tag{1}$$

Where U is the strain energy expressed by Eq. (2), defined by the integral of the specific strain energy u in an initial reference volume V. P is the potential energy of the external forces expressed by Eq. (3), in which the degrees of freedom, considering a plane frame element with two nodes and three degrees of freedom per node, can be represented by $X_i = (X_1, Y_1, \theta_1, X_2, Y_2, \theta_2)$ for $i = (1,2,3,4,5,6)$ and the respective nodal loads for the two degree of freedom represented by $F_i = (F_{X1}, F_{Y1}, M_{\theta 1}, F_{X2}, F_{Y2}, M_{\theta 2})$.

$$U = \int_V u dV = \int_V \int_\varepsilon \sigma \, d\varepsilon \, dV \tag{2}$$

$$P = \sum F_i X_i \tag{3}$$

in which σ represents the stress field according to the constitutive or rheological relation of the material as a function of the strain field ε.

Applying the principle of stationary total potential energy (Crisfield, 2003) in Eq. (1), one can obtain the equilibrium position of the structure from Eq. (4). So, the structure's equilibrium will occur when the derivative of this stationary total potential energy, in relation to the nodal parameters, is null, that is, when the variation rate of the total potential energy is null.

$$\frac{d\Pi}{dX_i} = \frac{dU}{dX_i} - \frac{dP}{dX_i} = 0 \tag{4}$$

The Equation (4) is a system of six equations (three degrees of freedom to each one of the two nodes that define a frame element) and represents a nonlinear system of equations. As the relationship between the total strain energy, U, and nodal parameters, X_i, is nonlinear. Then, it must be solved using a proper method to solve systems of equations. Furthermore, it should be adopted a constitutive or rheological relation in Eq. (2) which represents appropriately the behavior of the material.

2.1 Definition of the rheological relation

One of the main characteristics in a physically nonlinear analysis is the adoption of a constitutive or rheological relation that represents, in an appropriate way, the behavior of the material. Therefore, following Mesquita and Coda (2003) and Panagiotopoulos et al. (2014), the rheological relation that represents the viscoelastic behavior of a material is deduced from a rheological model. The choice of an adequate rheological model was based on the expected behavior for the creep phenomenon in solid materials. Having this in mind, the general uniaxial Maxwell rheological model in parallel was adopted. This model, according to Findley et al. (1976), can be obtained by parallel association between an elastic model and many Maxwell arms, Fig. 1-a. The used model was restricted to one Maxwell arm (a series of one elastic element with a viscous element) in parallel with an elastic arm (Hooke model), resulting in the model presented in Fig. 1-b. This model is also known as standard solid model or Zener model.

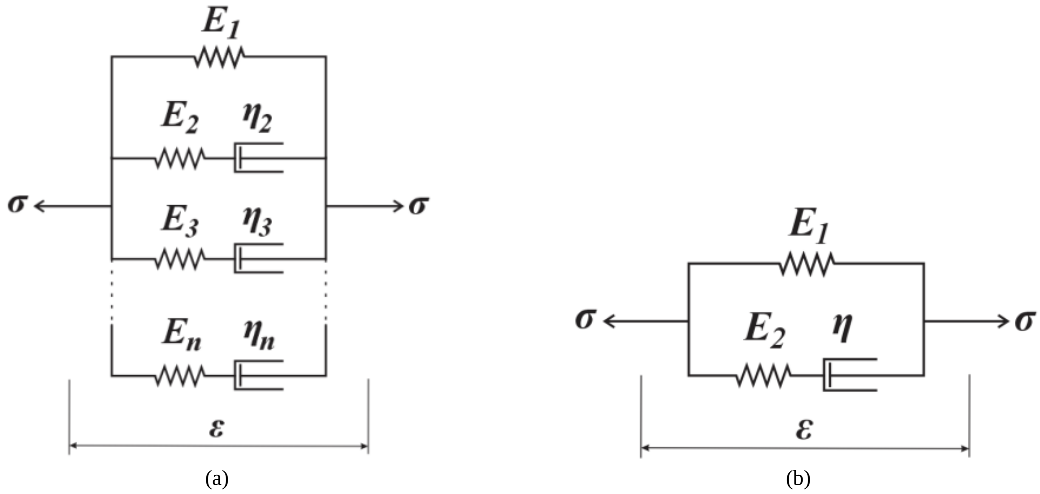

Figure 1. (a) Generalized Maxwell model in parallel; (b) Standard solid model

As it is shown in Marques and Creus (2012), the rheological relation of the standard solid model present in Fig. 1-b can be represented by the following expression:

$$\sigma = E_1\varepsilon + \frac{\eta(E_1 + E_2)\dot{\varepsilon}}{E_2} - \frac{\eta\dot{\sigma}}{E_2} \tag{5}$$

Where σ and ε represent, respectively, the normal stress and linear strain, and $\dot{\sigma}$ and $\dot{\varepsilon}$ represent, respectively, the variation rates of stress and strain over time. The terms E_1, E_2 and η are the parameters of the elements described in Fig. 1-b, and represent the properties of the material. The immediate elastic behavior depends on parameters E_1 and E_2, where the sum of these parameters represents the elasticity module of the material. Moreover, parameter E_1 determines the final strain (the sum of the immediate elastic strain and the damped elastic strain), after a considerably long time interval, and represents the elasticity module of the material in the damped elastic behavior. Parameter η represents viscosity module of the material, which determines the strain rate over time and provides a damped behavior to the material.

Equation (5) can be simplified to represent the uniaxial rheological relation of the viscoelastic material in the case of creep phenomenon, neglecting the term for the rate of stress variation over time. This equation can be used in Eq. (2) to obtain the total strain energy. To do so, knowing the properties of the material, it is necessary to define an adequate strain measure in relation to the implemented finite element.

2.2 Particularization of the strain measure

From the general formulation and the rheological relation of item 2.1 it's possible to describe the nonlinear positional Formulation of the Finite Elements Method, applied to the creep behavior description in frame elements, particularizing the strain measure in a way that is adequate to the implemented element.

Aiming to particularize the strain measure is necessary to understand the geometry of the element to be studied and its relation with the adopted strain measure. So, in this formulation each finite element has its geometry mapped out by the parametrization in function of the dimensionless variable ξ (ranging from 0 to 1) as shown in Fig. 2. Where X_1, Y_1, θ_1, X_2, Y_2 and θ_2 are the nodal parameters of the finite element and represent the degrees of freedom in each node.

Accordingly it is possible to define the position of each point of the element and, as a consequence, the geometry in function of the nodal parameters by using Eqs. (6) – (9).

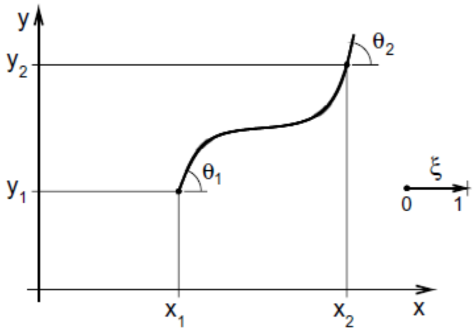

Figure 2. Parametrized geometry (Coda and Greco, 2004)

$$l_x = (X_2 - X_1) \tag{6}$$

$$l_y = (Y_2 - Y_1) \tag{7}$$

$$x = X_1 + l_x\xi \tag{8}$$

$$y = c\,\xi^3 + d\,\xi^2 + e\,\xi + f \tag{9}$$

It is necessary to define the parameters *c*, *d*, *e* and *f* in this last based on the nodal coordinates. Then, considering the boundary conditions in Eq. (9), we have:

$$y_{(\xi=0)} = f = Y_1 \tag{10}$$

$$\left.\frac{dy}{d\xi}\right|_{\xi=0} = e = \left.\frac{dy}{dx}\frac{dx}{d\xi}\right|_{\xi=0} = tan(\theta_1)l_x \tag{11}$$

$$\left.\frac{dy}{d\xi}\right|_{\xi=1} = 3c + 2d + e = \left.\frac{dy}{dx}\frac{dx}{d\xi}\right|_{\xi=1} = tan(\theta_2)l_x \tag{12}$$

$$y_{(\xi=1)} = c + d + tan(\theta_1)l_x + Y_1 = Y_2 \tag{13}$$

From Eqs. (12) and (13):

$$c = (tan(\theta_2) + tan(\theta_1))l_x - 2l_y \tag{14}$$

$$d = 3l_y - (tan(\theta_2) + 2tan(\theta_1))l_x \tag{15}$$

The engineering strain measure as defined in Ogden (1997) can be represented by:

$$\varepsilon = \frac{ds - ds_0}{ds_0} = \frac{\frac{ds}{d\xi} - \frac{ds_0}{d\xi}}{\frac{ds_0}{d\xi}} \tag{16}$$

Where *ds* represents the length of a given fiber of the body (parallel to the central axis) in a deformed configuration and ds_0 represents its length in a non-deformed configuration.

For Central Line (CL) fiber that passes by the element's geometric center, we can define:

$$\left.\frac{ds_0}{d\xi}\right|_{CL} = \sqrt{\left(\frac{dx_0}{d\xi}\right)^2 + \left(\frac{dy_0}{d\xi}\right)^2} = \sqrt{\left(l_{x_0}\right)^2 + \left(l_{y_0}\right)^2} = l_0 \tag{17}$$

$$\left.\frac{ds}{d\xi}\right|_{CL} = \sqrt{\left(\frac{dx}{d\xi}\right)^2 + \left(\frac{dy}{d\xi}\right)^2} = \sqrt{(l_x)^2 + (3c\xi^2 + 2d\xi + e)^2} \tag{18}$$

This way, the central line strain can be defined by using Eqs. (16), (17) and (18) as in:

$$\varepsilon_{CL} = \frac{\sqrt{(l_x)^2 + (3c\xi^2 + 2d\xi + e)^2} - l_0}{l_0} = \frac{1}{l_0}\sqrt{(l_x)^2 + (3c\xi^2 + 2d\xi + e)^2} - 1 \quad (19)$$

According to Bernoulli-Euler kinematics we can describe the strain in any given fiber of the finite element due to the strain and curvature of the fiber that passes by the central line, as shown in Eq. (20). For this, it is necessary to adopt a coordinate *z*, orthogonal to the central line, which defines the distance of any given fiber from the central line.

$$\varepsilon = \varepsilon_{CL} + \kappa z \quad (20)$$

in which κ represents the element's curvature, defined according to Wylie and Barrett (1995), due to the dimensionless variable ξ. This curvature can be represented by:

$$\kappa = \frac{\frac{dx}{d\xi}\frac{d^2y}{d\xi^2} - \frac{d^2x}{d\xi^2}\frac{dy}{d\xi}}{\left(\sqrt{\left(\frac{dx}{d\xi}\right)^2 + \left(\frac{dy}{d\xi}\right)^2}\right)^3} = \frac{l_x(6c\xi + 2d)}{\left(\sqrt{(l_x)^2 + (3c\xi^2 + 2d\xi + e)^2}\right)^3} \quad (21)$$

From Eqs. (19), (20) and (21) we can define the normal strain of any given fiber, due to ξ, *z* and nodal parameters X_1, Y_1, θ_1, X_2, Y_2 and θ_2 that define parameters *c*, *d*, *e* and *f*.

By using Eqs. (2) and (5), after neglecting the term for the rate of stress variation over time, the total strain energy can be expressed in:

$$U = \int_V \int_\varepsilon \left(E_1\varepsilon + \frac{\eta(E_1 + E_2)}{E_2}\dot{\varepsilon}\right) d\varepsilon\, dV \quad (22)$$

By defining the strain rate ($\dot{\varepsilon}$) through the chain rule, using the derivative in relation to the degrees of freedom, we have:

$$\dot{\varepsilon} = \frac{d\varepsilon}{dt} = \frac{d\varepsilon}{dX_i}\frac{dX_i}{dt} = \varepsilon_{,i}\dot{X}_i \quad (23)$$

Where $\dot{X}$ represents the velocity of the positional variation in the direction of each one of the six degrees of freedom (X_1, Y_1, θ_1, X_2, Y_2 and θ_2) and $\varepsilon_{,i}$ is the derivative of Eq. (20) in relation to the degrees of freedom.

Working with a change of variables, the integral of the second term of Eq. (22) can be represented in relation to degrees of freedom. To do so, Eq. (20) is used in the following relation between $d\varepsilon$ e dX_i:

$$d\varepsilon = \varepsilon_{,i}\, dX_i = (\varepsilon_{LC,i} + \kappa_{,i}\, z)dX_i \quad (24)$$

By substituting Eqs. (20), (23) and (24) in Eq. (22) and evaluating the integral of the first term in relation to the strain (ε), the total strain energy becomes:

$$U = \int_V \left[\frac{E_1}{2}({\varepsilon_{CL}}^2 + 2\varepsilon_{CL}\kappa z + \kappa^2 z^2) + \right.$$

$$+\int_{X_i} \frac{\eta(E_1+E_2)}{E_2}({\varepsilon_{CL},_i}^2 + 2\varepsilon_{CL},_i\,\kappa,_i\,z + {\kappa,_i}^2\,z^2)\dot{X}_i dX_i\Bigg] dV \tag{25}$$

Using the parametrization of the finite element in the dimensionless variables ξ and λ, Fig. 3, the integral in relation to the volume in Eq. (25) can be evaluated in relation to the parametrized length and height, as shown in Eq. (26), taking into account that the area of cross section of the element is constant over the length.

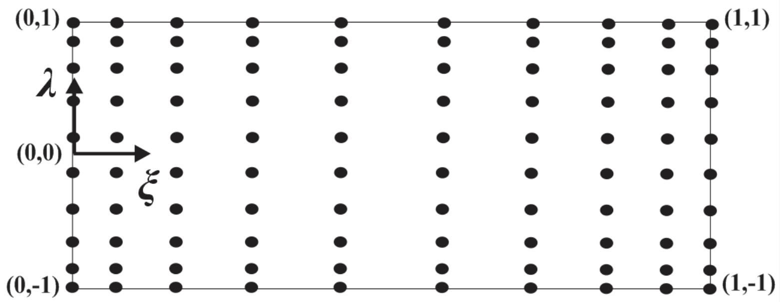

Figure 3. Parametrization of the finite element with the help of dimensionless variables at height (λ) and length (ξ)

$$U = \int_0^1 \int_{-1}^1 l_0 h_\lambda b_\lambda \Bigg[\frac{E_1}{2}({\varepsilon_{CL}}^2 + 2\varepsilon_{CL}\kappa z + \kappa^2 z^2) + \\ + \int_{X_i} \frac{\eta(E_1+E_2)}{E_2}({\varepsilon_{CL},_i}^2 + 2\varepsilon_{CL},_i\,\kappa,_i\,z + {\kappa,_i}^2\,z^2)\dot{X}_i dX_i\Bigg] d\lambda d\xi \tag{26}$$

The parametrization in relation to the height was introduced with the objective of enabling the analysis of bending creep behavior from the fitting of the model based on uniaxial tension creep behavior and uniaxial rheological relations. Then, a beam that is exposed to bending can be idealized as a superposition of bars (a bundle of bars), where the number of bars is equal to the number of Gauss points distributed over the height. Each one of these bars, with the centroid located in a Gauss point at λ, is exposed either to tension or compression, depending on its location in relation to the central line. The height (h_λ) and the base (b_λ) of each bar are defined by the localization of its respective Gauss point and by the geometry of the beam.

Equation (26) defines the total strain energy in function of the physical properties of the material, the geometrical properties of the element and the nodal parameters, in a complete way, except for the velocity of position variation in the direction of each degree of freedom $\dot{X}_i$, which will be defined in the following item in function of the dimensionless variable ξ and the nodal parameters.

Using Eqs. (3) and (26) in Eq. (4), which represents the application of the principle of stationary total potential energy, it is possible to obtain the solution for the system that provides the position of equilibrium for a structure, discretized in frame elements and exposed to a state of specific static load, considering the contribution of the material's viscoelastic behavior. Since Eq. (4) represents a nonlinear system of equation, it can be solved using the method of Newton-Raphson, in a procedure similar to the ones presented in Becho et al. (2015).

2.3 Representation of the velocities of position variation in the direction of the degrees of freedom

We start by defining positions *x* and *y* of a given point of the finite element by using Eqs. (8) and (9). In a similar way, in the case of spin θ in a given cross section, defined by ξ, taking into account the parametrized geometry of the element, Fig. 2, we have:

$$\frac{dy}{dx}\frac{dx}{d\xi} = 3c\xi^2 + 2d\xi + e = \tan(\theta) l_x \tag{27}$$

$$\theta = \arctan\left(\frac{3c\xi^2 + 2d\xi + e}{l_x}\right) \tag{28}$$

Where *c*, *d* and *e* can be defined by Eqs. (11), (14) and (15).

Using Eqs. (8), (9) and (28) it is possible to obtain the differences in position *x*, *y* and θ between a Gauss point (ξ_m) and the previous Gauss point (ξ_{m-1}), defining segments of the finite element with specific dimensions and orientations. Finally, the velocity of the position variation ($\dot{X}_i$) in each Gauss point in the direction of each one of the six degrees of freedom, eliminating the rigid body motions of the element, can be obtained through the variation of these position differences in relation to the initial (non-deformed) and current (deformed) configurations. This means that the velocities of position variation in each Gauss point are defined by the variations in the dimension and orientation of the comprehended segment between this Gauss point and the previous Gauss point in a time interval. So, for a particular Gauss point ξ_m in the direction of a degree of freedom X_1, we have:

$$\dot{X}_1 = \frac{[x(\xi_m) - x(\xi_{m-1})] - [x^0(\xi_m) - x^0(\xi_{m-1})]}{\Delta t} \tag{29}$$

In which Δt represents the necessary time interval for the element to go from the initial position (indicated by the parameter with superscript "0") to the final position (indicated by the parameter without superscript). Similarly to the one in Eq. (29), it is possible to define the velocity of position variation in the direction of each degree of freedom, $\dot{X}_i$, to be used in Eq. (26).

3 MODEL FITTING

Taking into account the approach used in the formulation described in item 2, where the beam is idealized as a bundle of bars, a simple fitting can be adopted based on the uniaxial creep test results in bars exposed to tension. These results, obtained in the literature (Youssef, 2010), refer to the simulations of creep in Glass Fiber Reinforced Plastic (GFRP) pultruded bars, made of high-strength E-glass fiber (77% per volume) impregnated in vinylester resin. The bars are one meter long, the circular cross section area is 70.88×10^{-6} m^2 and the elasticity module is equal to 46.9 GPa. The tests were based on the obtainment of the bars' creep strains, over a period of 10000 hours, exposed to constant uniaxial stress in four different levels of stress (15%, 30%, 45% and 60% in relation to the ultimate stress of the material, which is of 854 MPa).

The bar was discretized in the numerical model by one frame element that was fixed at one end and simply supported at the other, as shown in Fig. 4.

Figure 4. Bar exposed to tension

The loads were applied to the supported end and refer to the tension loads that provide the four simulated levels of stress. The experimental results, in the four levels of stress, are represented by the discrete points in Fig. 5.

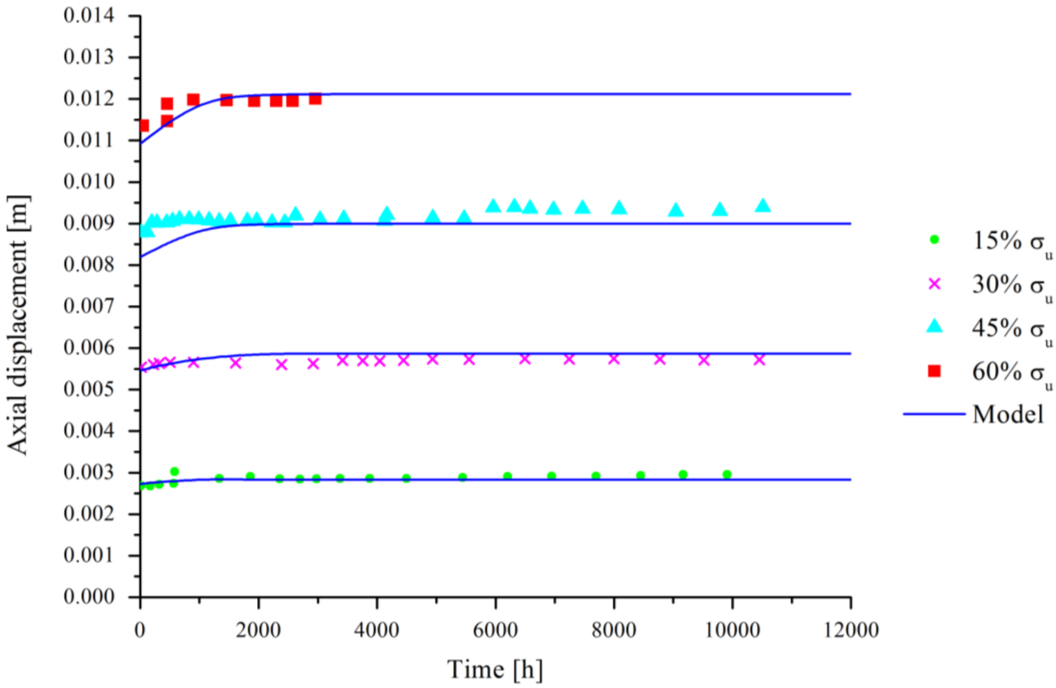

Figure 5. Numerical and experimental axial displacements

The developed calibration of the formulation was done by obtaining the relation between the viscosity module (η) and the stress level (σ) to which the material was exposed. So, from the fitting of the viscosity module to each stress level, a quadratic regression was performed, using the least squares method and obtaining the following relation:

$$\eta = 1.4746 \cdot 10^{4}|\sigma| - 0.1295 \cdot 10^{-4}\sigma^{2} \tag{30}$$

Where $|\sigma|$ represents the absolute value of stress level. Accordingly it was considered that the material presents the same viscosity properties both in the behavior under tension and the behavior under compression.

The relations between the elasticity modules (E_1 and E_2) of the adopted rheological module and the elasticity module (E) of the material were obtained so that it provides the best fit with the experimental results. So, for the adopted material and for the four levels of stress, E_1 corresponds to 90% of E, and E_2 corresponds to 10% of E.

The numerical results obtained by the fitted formulation, substituting Eq. (30) in Eq. (26), are represented in Fig. 5 by the continuous lines in the four levels of stress. These results show the fitting capacity of the formulation and provide a coefficient of determination (R^2) equal to 94%.

For the beams exposed to bending, since the contribution of creep in the behavior of the material is directly connected to the stress level to which the material is exposed, using Eq. (30) it is possible to obtain the variation of the viscosity module over the height of the beam (or the value of the viscosity module in each bar of the idealized bundle) through the stress profile developed due to the bending effort.

4 NUMERICAL EXAMPLES

4.1 Simply supported beam with concentrated load

The first numerical example is a simply supported GFRP beam with concentrated load applied to the center of the span, as shown in Fig. 6-a. The goal of this example was to compare the numerical result of the viscoelastic behavior by using the fitted formulation with the analytical result of the elastic behavior. These results were based on the midspan deflection measure over time (vertical displacement). The numerical result was obtained through computational implementation of the presented formulation. This implementation was based on the method of Newton-Raphson to solve the nonlinear system of equations described by Eq. (4) and in numerical integrations with ten Gauss points, both for the height and length of each finite element, to develop Eq. (26).

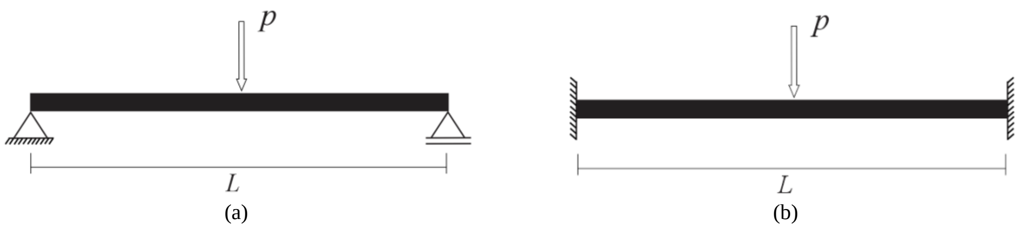

Figure 6. (a) Simply supported beam; (b) Fixed beam

The beam illustrated by Fig. 6-a shows a free span (L) equal to 5 m and was discretized into ten finite elements, each one with 0.5 m of length. The cross section of each one has area of 15.0×10^{-3} m^2 and the moment of inertia of 28.13×10^{-6} m^4. The elasticity modules are E_1 = 42.21 GPa, E_2 = 4.69 GPa. The viscosity module is defined by the function for the stress level using Eq. (30).

The load (p) was applied to the midspan in one single step and has intensity of 10000N. The analysis was performed considering ten steps of time of Δt = 1000 hours, coming to a total of 10000 hours.

The numerical results for the viscoelastic behavior are exposed in Fig. 7-a. The analytical result for the elastic case (Leet et al., 2011) was obtained by using Eq. (31) and provided a midspan deflection value equal to 19.7×10^{-3} m. The non-deformed geometry and the deformed geometries for the elastic and viscoelastic behaviors are illustrated in Fig.7-b.

$$Maximum\ deflection = \frac{pL^3}{48(E_1+E_2)I} \tag{31}$$

It is possible to observe from Fig. 7 that the code could describe the creep behavior (increase of the strain over time under constant stress) and that this behavior, for the properties of the adopted material, could cause strains increasing depending on the applied loads and the geometry of the structure. In this example, the beam presented a maximum numerical viscoelastic deflection of 27.4×10^{-3} m during a period of approximately 6000 hours, around 40% bigger than the analytical elastic deflection.

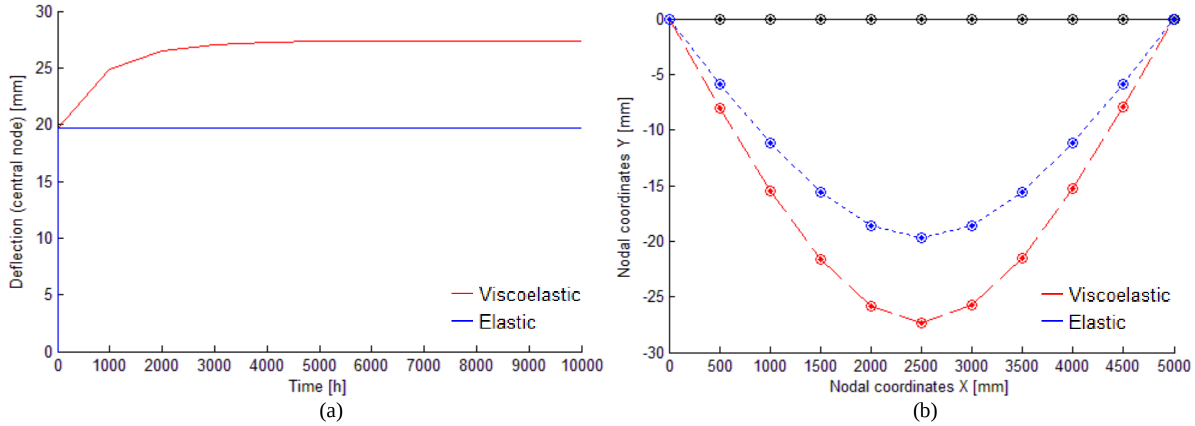

Figure 7. (a) Evolution of the deflection over time on the simply supported beam; (b) Deformed geometry of the simply supported beam

4.2 Fixed beam with concentrated load

The second numerical example is a fixed GFRP beam, shown in Fig. 6-b, with a concentrated load applied to center of the span and with the same data for load, material, geometry and discretization of the previous example, as well as the strategy adopted for the analysis. The goal of this example is to compare the contribution of creep to the deflection at the midspan with a change in the support in relation to the previous example.

The numerical results for the viscoelastic behavior are shown in Fig. 8-a. The analytical result for the elastic case (Leet et al., 2011) was obtained through Eq. (32) and provided a midspan deflection value equal to 4.9×10^{-3} m. The non-deformed geometry and the deformed geometries for the elastic and viscoelastic behavior are illustrated in Fig. 8-b.

$$Maximum\ deflection = \frac{pL^3}{192(E_1 + E_2)I} \tag{32}$$

From the presented results it is possible to observe that for the fixed beam the contribution of creep was less apparent than it was in the simply supported beam. This is mainly due to the difference in the distribution of the stress over the beams in the two examples, a consequence of the distribution of the internal bending efforts and the fact that the viscoelastic behavior is related to the stress level to which the material is exposed.

In this last example, the beam presented a maximum numerical viscoelastic deflection of 5.1×10^{-3} m in a period of approximately 2000 hours, around 4% bigger than the maximum analytical elastic deflection.

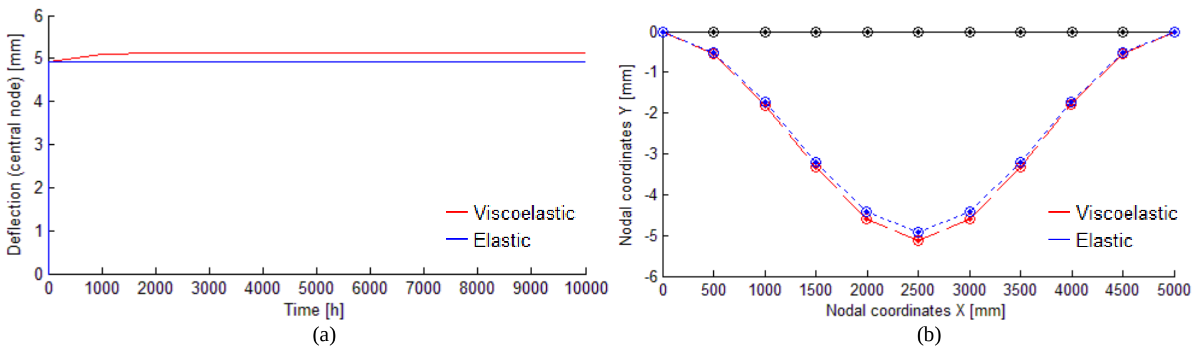

Figure 8. (a) Evolution of the deflection over time on the fixed; (b) Deformed geometry of the fixed beam

5 CLOSING REMARKS

The purpose of this work was to present the formulation developed to describe the mechanical viscoelastic behavior in beams, more specifically the creep phenomenon. This developed formulation was based on the nonlinear positional formulation of the Finite Elements Method and on a parametrization approach of the beam height that enables the creep consideration. From the results obtained in the presented examples, the formulation was capable of representing the evolution of the displacements of the beams over time under static load, presenting displacement profiles and equilibrium positions as expected from the theory of viscoelasticity. Moreover, the proposed parametrization approach made it possible to perform the model fitting to the adopted material in a simple way, through the creep results of uniaxial tension tests on the bars. However, to confirm the achieved results, it was necessary to perform creep tests of bending on beams made of the same fitted material.

Analyzing the presented examples we could verify that the creep phenomenon can occur in a more apparent way depending on the boundary conditions and the geometry of the structure, due to levels and distribution of the given stress. Moreover, still based on the analyzed examples, it’s possible to note that the effects of creep may cause additional significant displacements in structures exposed to constant loads, according to what was pointed out by the researches mentioned in this paper. So, depending on the application, work conditions, and the adopted safety and design tolerances, the creep phenomenon cannot be neglected, since it may cause failures in long periods of exposition to a stress quite inferior to the stress limit of the material.

ACKNOWLEDGEMENTS

The authors would like to acknowledge CNPq (National Council of Scientific and Technological Development), CAPES (Coordination of Improvement of Higher Education Personnel), FAPEMIG (Minas Gerais State Research Foundation) and PROPEEs/UFMG (Structure Engineering Graduate Program of the Federal University of Minas Gerais) for financial supports.

REFERENCES

Bahraini, S. M. S., Eghtesad, M.,Farid, M., Ghavanloo, E., 2013. Large deflection of viscoelastic beams using fractional derivative model. *Journal of Mechanical Science and Technology*, v. 27, n. 4, p. 1063-1070.

Becho, J. S., Barros, F. B., Greco, M., 2015. Positional formulation for creep mechanical behavior of beams and framed structures. *Science & Engineering Journal*, v. 24, n. 1, p. 31-41. (in Portuguese)

Carniel, T. A., Muñoz-Rojas, P. A., Vaz, M., 2015. A viscoelastic viscoplastic constitutive model including mechanical degradation: Uniaxial transient finite element formulation at finite strains and application to space truss structures. *Applied Mathematical Modelling*, v. 39, n. 5, p. 1725-1739.

Christensen, R. M., 2010. *Theory of viscoelasticity*. Dover Publications, New York.

Coda, H. B., Greco, M., 2004. A simple FEM formulation for large deflection 2D frame analysis based on position description. *Computer Methods in Applied Mechanics and Engineering*, v. 193, n. 33, p. 3541-3557.

Crisfield, M. A., 2003. *Non-linear finite element analysis of solids and structures*. v.1. John Wiley & Sons, West Sussex.

Findley, W. N., Lai, J. S., Onaran, K., 1976. *Creep and relaxation of nonlinear viscoelastic materials*. Dover Publications, New York.

Godat, A., Légeron, F., Gagné, V., Marmion, B., 2013. Use of FRP pultruded members for electricity transmission towers. *Composite Structures*, v. 105, p. 408-421.

Haveroth, T. C. C., Muñoz-Rojas, P. A., Kühl, A., Sasse, F. D., 2015. Modeling HDPE nonlinear viscoelastic behavior using fractional derivatives: parameters interpolation and economy schemes. In: *V International Symposium on Solid Mechanics*, Belo Horizonte, Brazil.

Kaliske, M., Rothert, H., 1997. Formulation and implementation of three-dimensional viscoelasticity at small and finite strains. *Computational Mechanics*, v. 19, n. 3, p. 228-239.

Kästner, M., Obst, M., Brummund, J., Thielsch, K., Ulbricht, V., 2012. Inelastic material behavior of polymers–experimental characterization, formulation and implementation of a material model. *Mechanics of Materials*, v. 52, p. 40-57.

Kühl, A., Muñoz-Rojas, P. A., Vaz, M.,Carniel, T. A., 2013. Modeling nonlinear viscoelastoplastic behavior or high density polyethylene (HDPE) using particle swarm optimization (PSO). In: *XXXIV Iberian Latin-American Congress on Computational Methods in Engineering*. Pirenópolis, Brazil.

Leet, K.,Uang, C. M., Gilbert, A., 2011. *Fundamentals of structural analysis*. 4.ed. McGraw-Hill, New York.

Liu, H., Polak, M., Penlidis, A., 2008. A practical approach to modeling time-dependent nonlinear creep behavior of polyethylene for Structural applications. *Polymer Engineering and Science*, v. 48, n. 1, p. 159-167.

Marques, S. P. C., Creus, G. J., 2012. *Computational viscoelasticity*. Springer, Heidelberg.

Mesquita, A. D., Coda, H. B., 2003. A simple Kelvin and Boltzmann viscoelastic analysis of three-dimensional solids by the boundary element method. *Engineering Analysis with Boundary Elements*, v. 27, n. 9, p. 885-895.

Muñoz-Rojas, P. A., Mendonça, P. T. R., Benvenutti, I. J., Creus, G. J., 2011. Modeling nonlinear viscoelastic behavior of High Density Polyethylene (HDPE): application of stress-time equivalence versus interpolation of rheological properties. In: *III International Symposium on Solid Mechanics*. Florianópolis, Brazil.

Ogden, R. W., 1997. *Non-linear elastic deformation*. Chichester, Ellis Horwood.

Panagiotopoulos, C. G., Mantič, V., Roubíček, T., 2014. A simple and efficient BEM implementation of quasistatic linear visco-elasticity. *International Journal of Solids and Structures*, v. 51, n. 13, p. 2261-2271.

Pérez Zerpa, J. M., Canelas, A., Sensale, B, Bia Santana, D., Armentano, R. L., 2015. Modeling the arterial wall mechanics using a novel high-order viscoelastic fractional element. *Applied Mathematical Modelling*, v. 39, n. 16, p. 4767-4780.

Sá, M. F., Gomes, A. M.,Correia, J. R., Silvestre, N., 2011. Creep behavior of pultruded GFRP elements–Part 1: Literature review and experimental study. *Composite Structures*, v. 93, n. 10, p. 2450-2459.

Semptikovski, S. C., Muñoz-Rojas, P. A., 2013. A Geometrically Nonlinear Simplified Beam Element with Linear Viscoelastic Behaviour. In: *IV International Symposium on Solid Mechanics*, Porto Alegre, Brazil.

Shen, J. J., Li, C. G., Wu, H. T., Kalantari, M., 2013. Fractional order viscoelasticity in characterization for atrial tissue. *Korea-Australia Rheology Journal*, v. 25, n. 2, p. 87-93.

Wylie, C. R., Barrett, L. C., 1995. *Advanced engineering mathematics*. 6.ed. McGraw-Hill, New York.

Youssef, T. A., 2010. *Time-dependent behavior of fibre reinforced polymer (FRP) bars and FRP reinforced concrete beams under sustained load*. Ph.D. thesis, University of Sherbrooke, Sherbrooke, Canada.